

A COMPARISON OF ENERGY TRANSPORT MEASUREMENTS AND COMPUTER SIMULATIONS IN A SINGLE MODULE PROTOTYPE FOR PBFA II*

E. L. Neau, J. F. Seamen, D. D. Bloomquist,
S. R. Babcock, L. X. Schneider and B. R. Sujka
Sandia National Laboratories
Albuquerque, New Mexico

Abstract

The 36-module Particle Beam Fusion Accelerator (PBFA II)¹ is designed to provide a 30 MV pulse, with greater than 150 TW, to a centrally located lithium ion diode. Each module is driven by a 6 MV, 400 kJ Marx generator and uses three water-insulated and switched pulse compression stages followed by a voltage inversion-adder unit. An impedance matching transmission-line transformer couples the output pulse from the inversion-adder unit to the central vacuum insulator, plasma erosion switches, and ion diode. The prototype of a single PBFA-II module, called Demon, is being used to test component design, including a mock-up of a section of the vacuum insulator, and to determine overall module operating characteristics. This paper presents the results of measurements of energy transport efficiencies through the successive pulse compression stages. Results of energy transport measurements on an 18 module, one-fifth scale model, are also compared to the single-line data. We present a comparison of measured parameters with computer circuit code simulations of the hardware design. Comparisons are used to suggest areas of possible improvements. The measured module output characteristics agree with the code simulations and meet the design requirements for the PBFA-II accelerator.

Introduction

The Demon prototype module for PBFA-II is shown in Figure 1. This section of the paper will give a brief overview of the physical and electrical characteristics of the Demon module. Following sections address energy transport simulations and measurements in the gas switch region and in the output transmission-line transformers. A final section presents a comparison of measured module parameters with the results obtained with a circuit code model developed from the physical geometry.

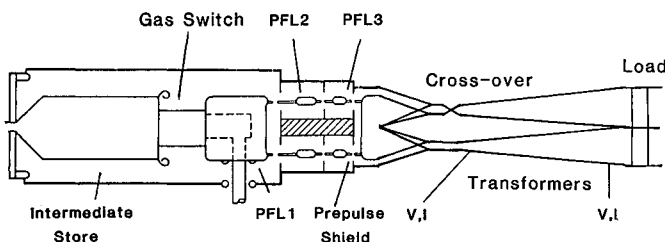


Figure 1. Cross-sectional view of Demon pulse compression section.

The primary energy storage unit is a Marx generator which consists of 30 stages, each with two plus-minus charged 100 kV capacitors, with an erected capacity of 22.3 nF. The Marx is charged to 95 kV, at the nominal operating point, and stores 362 kJ. The Marx energy can be dumped to a 22 ohm resistive load for maintenance and testing purposes.

The energy from the erected Marx generator is transferred, in the PBFA II accelerator, to a coaxial 3.8 ohm water-insulated intermediate storage capacitor (ISC) with an electrical length of 66 nS. The useable capacity of the ISC is 14.6 nF. In addition, approximately 1.2 nF appears across the gas switch to the first pulse-forming line (PFL1) and the energy stored in this capacity is internally dissipated in the gas switch when the switch closes.

*This work supported by the United States Department of Energy under Contract number DE-AC04-DP00789.

The stored energy is switched out of the ISC by a laser-triggered, multi-section, SF₆ insulated spark gap switch called Rimfire³. This switch, located in the deionized water environment, is designed for multi-channel operation and small overall size, obtained through uniform field grading, to achieve a low-inductance geometry of 300 nH. This switch has a triggered operating point of 5 to 5.2 MV. The low gas-switch inductance is required to achieve charging of the first coaxial pulse-forming line (PFL1) in the double-bounce charging mode (DBCM)⁴. In this mode, the risetime of the voltage wave launched into PFL1, when the Rimfire switch closes, is the same as the two way transit time of the PFL1. The DBCM reduces the required switch hold-off time and gap length for the self-closing water switches located between the first and second pulse-forming lines as shown in Figure 1. The required hold-off voltage and time of the first set of water gaps would be over 10 MV and several hundred nanoseconds with conventional resonant (1-cos) charging, but drops to 5 MV and 75 ns with double-bounce charging. The reduced hold-off of 5 MV requires a de-enhanced switch point spacing of 10 cm. A 10 MV holdoff would be impossible to achieve since the switch gap spacing would approach the size of the interline spacing. The reduced spacing also minimizes energy losses in the average resistance of 40 milliohms-per-cm of gap length of the water breakdown channel^{5,6}. Four switch sites, with 10 cm gaps and 35.5 cm long switch rods, are used to obtain approximately 100 nH of inductance between PFL1 and PFL2. The PFL1 has an impedance of 3.89 ohms and an electrical one-way length of 36 ns.

The second pulse-forming line (PFL2), configured in a triaxial geometry, has an impedance of 2.16 ohms and an electrical one-way length of 20 ns. Triaxial geometry is used to minimize effects of stray capacity on output pulse shape. PFL2 also uses the DBCM. Eight water switch sites are used between PFL2 and PFL3 with a gap spacing of 3 cm and a switch rod length of 23.7 cm.

The third triaxial pulse-forming line, PFL3, also has an impedance of 2.16 ohms and serves to reduce downline prepulse. Eight water switches, with 0.25 cm gaps and 26.4 cm long rods, isolate PFL3 from the following coaxial section.

The sheet-metal convolute, which follows PFL3, converts the triaxial pulse-forming line geometry to a coaxial geometry and then to two parallel-plate outputs, each with a nominal impedance of 4.3 ohms.

A crossover assembly, consisting of 9 rods alternately connecting upper and lower plates, is placed in one set of output lines to spatially invert the electric field vector and allow voltage addition of the upper and lower forward-going pulses at the vacuum-insulator stack. The crossover assembly region is followed by two sets of late-time energy diverter salt-solution resistors in both the upper and lower transmission lines. The salt-solution resistor end caps are separated by a water gap of 5.7 cm which is designed to close on pulses reflected from the impedance of the vacuum insulator stack, plasma erosion switch, and ion-diode load. The combined resistance in each transmission line matches the line impedance of 4.3 ohms and can dissipate 40 kJ of reflected and late-time energy. A spring-loaded short circuit can be placed between the resistors so that they also function as dummy-load resistors, absorbing the full 360 kJ module energy, for downline module testing.

Report Documentation Page			Form Approved OMB No. 0704-0188	
<p>Public reporting burden for the collection of information is estimated to average 1 hour per response, including the time for reviewing instructions, searching existing data sources, gathering and maintaining the data needed, and completing and reviewing the collection of information. Send comments regarding this burden estimate or any other aspect of this collection of information, including suggestions for reducing this burden, to Washington Headquarters Services, Directorate for Information Operations and Reports, 1215 Jefferson Davis Highway, Suite 1204, Arlington VA 22202-4302. Respondents should be aware that notwithstanding any other provision of law, no person shall be subject to a penalty for failing to comply with a collection of information if it does not display a currently valid OMB control number.</p>				
1. REPORT DATE JUN 1985	2. REPORT TYPE N/A	3. DATES COVERED -		
A Comparison Of Energy Transport Measurements And Computer Simulations In A Single Module Prototype For PBFA II			5a. CONTRACT NUMBER	
			5b. GRANT NUMBER	
			5c. PROGRAM ELEMENT NUMBER	
6. AUTHOR(S)			5d. PROJECT NUMBER	
			5e. TASK NUMBER	
			5f. WORK UNIT NUMBER	
7. PERFORMING ORGANIZATION NAME(S) AND ADDRESS(ES) Sandia National Laboratories Albuquerque, NM 87185			8. PERFORMING ORGANIZATION REPORT NUMBER	
9. SPONSORING/MONITORING AGENCY NAME(S) AND ADDRESS(ES)			10. SPONSOR/MONITOR'S ACRONYM(S)	
			11. SPONSOR/MONITOR'S REPORT NUMBER(S)	
12. DISTRIBUTION/AVAILABILITY STATEMENT Approved for public release, distribution unlimited				
13. SUPPLEMENTARY NOTES See also ADM002371. 2013 IEEE Pulsed Power Conference, Digest of Technical Papers 1976-2013, and Abstracts of the 2013 IEEE International Conference on Plasma Science. Held in San Francisco, CA on 16-21 June 2013. U.S. Government or Federal Purpose Rights License.				
14. ABSTRACT The f6-module Particle Beam Fusion Accelerator (PBFA II) is designed to provide a 30 MV pulse, with greater than 150 TW, to a centrally located lithium ion diode. Each module is driven by a 6 MV, 400 kJ Marx generator and uses three water-insulated and switched pulse compression stages followed by a voltage inversion-adder unit. An impedance matching transmission-line transformer couples the output pulse from the inversion-adder unit to the central vacuum insulator, plasma erosion switches, and ion diode.				
15. SUBJECT TERMS				
16. SECURITY CLASSIFICATION OF:			17. LIMITATION OF ABSTRACT SAR	18. NUMBER OF PAGES 4
a. REPORT unclassified	b. ABSTRACT unclassified	c. THIS PAGE unclassified		

The late-time energy diverter resistors are followed by tapered flat-plate transmission-line transformers which are used to increase the energy which can be stored in the inductance inside the vacuum insulator stack. Energy is stored in this inductance during the conduction phase of the plasma erosion switch operation. The input impedance of the transformer section, for each of the two module outputs, is 4.3 ohms and the output impedance, where the transformer attaches to the vacuum insulator stack, is 12 ohms.

Local Impedance of Gas Switch Region

The Rimfire gas switch is located in a water filled coaxial geometry. This section presents an analysis of the results of time domain reflectometry (TDR) measurements of the impedance profile around the gas switch and demonstrates how this impedance affects the desired traveling-wave charging of PFL1. The forward going wave launched into PFL1 reflects off of the open circuit of the water switch pin area back towards the gas switch region. The 300 nH inductance presented by the closed geometry of the gas switch is intended to reflect the energy wave back towards the water switches. However, due to the low impedance of the water environment around the outside of the gas switch, energy leaks past the switch inductance back into the ISC and does not add to the forward going pulse. The original SCEPTRE⁷ model of the gas switch, based on an analysis of an equipotential plot from JASON⁸, is shown in Figure 2. The model was checked by injecting a pulse into PFL1 at the switch pin sites as shown in Figure 3. The results of the SCEPTRE simulation of this geometry did not match the measured results.

based on JASON calculations

1.2 nF

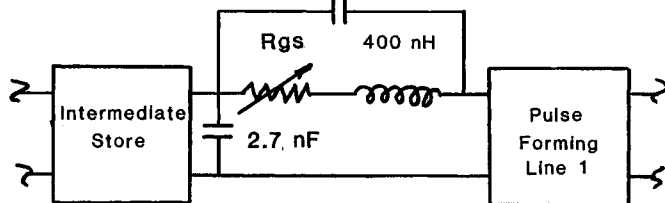


Figure 2. Original SCREAMER gas switch region model.

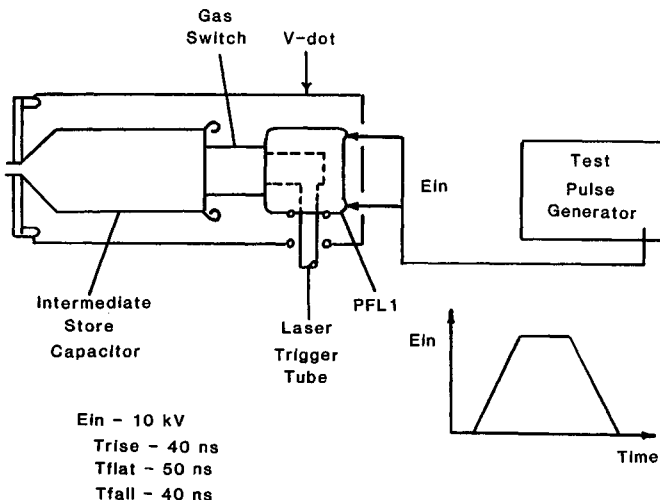


Figure 3. Gas switch time domain reflectometry geometry.

A transmission line model of the gas switch region was then constructed based on the dimensions of the region. This model is shown in Figure 4. The comparison between the measured waveform and the results of the two models are shown in Figure 5. The transmission line model gives a better representation of the actual behavior of the gas switch region. The improved transmission line model reduces the predicted forward going energy at the flat-plate outputs by 15 kJ. We have reduced the energy leakage in another module, called COMET⁹, by incorporating an oil filled cylinder around the gas switch to reduce the parallel capacity across the switch.

based on TDR measurements

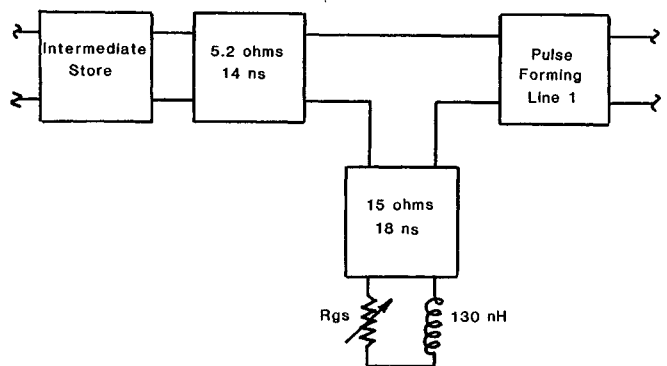


Figure 4. SCREAMER transmission line gas switch region model.

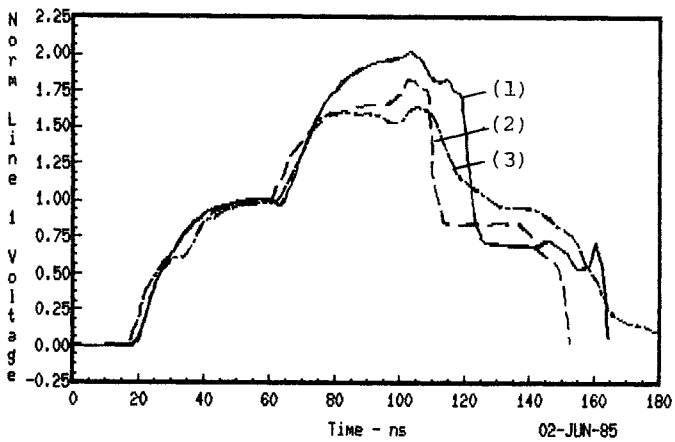


Figure 5. Demon line 1 TDR waveforms: 1) capacitive model, 2) transmission line model, and 3) measured Demon waveform.

Transformer Energy Transport Efficiency

The coaxial output of the Demon module is converted to two separate parallel plate outputs. One of these outputs is inverted so that the voltage outputs may be added at the vacuum stack assembly. The parallel plate output impedance is matched to the vacuum section impedance by tapered-impedance transmission-line transformers whose electrical length is 68 ns. An unexpected radiative-type energy loss mechanism has been identified, in our single module measurements, which occurs due to line-to-line coupling effects.

The transformer geometry is shown in Figure 1. Two series of measurements, using a fast 10 kV input pulse injected into the coaxial section towards the vacuum stack, have been made. One set of measurements was made with water over the bottom set of transformer lines (isolated case), and one set was made with water covering both sets of lines (coupled case). Voltage and current monitors were placed at the input and output of the lower transformer section to determine

transformer voltage gain and output impedance using a load-line plot.

The theoretical free space impedance profile of the isolated transformer section was calculated using the electro-static IMP code¹⁰. The SCREAMER circuit simulation code¹¹ was then used to calculate voltage gain and source impedance, using our measured input pulse. The calculated gain and impedance are within 5 percent of our measured values of 1.27 and 7.5 ohms. Predicted output pulse shape and pulse reflections at the input also agree with measured waveforms.

A calculation was made for the coupled case, using a similar electrostatic code. The results did not agree with the measured gain and source impedance. A series of impedance profiles between that of the isolated case and that of the coupled case were also tried without being able to match the measurements. A resistive loss was then added uniformly in parallel with the isolated case impedance profile from the IMP code in the SCREAMER simulation. The measured coupled voltage gain of 1.19 and output impedance of 8 ohms were matched when the total distributed loss resistance was set to 35 ohms. The load-line plots for the measurements, the distributed loss case, and the theoretical impedance profile are shown in Figure 6. This unwanted energy loss mechanism raises the output impedance by 7 percent and reduces the voltage gain by 7 percent. Both effects, in combination, reduce the output energy by 19 percent, compared to the isolated transformer case. The resistive loss model used here is an attempt to simulate a complex high-order mode excitation of the four-plate cavity formed by the transformers. Additional analysis will be required to understand the complex mode structure excited when the two sets of forward-going electromagnetic waves interact at the vacuum insulator.

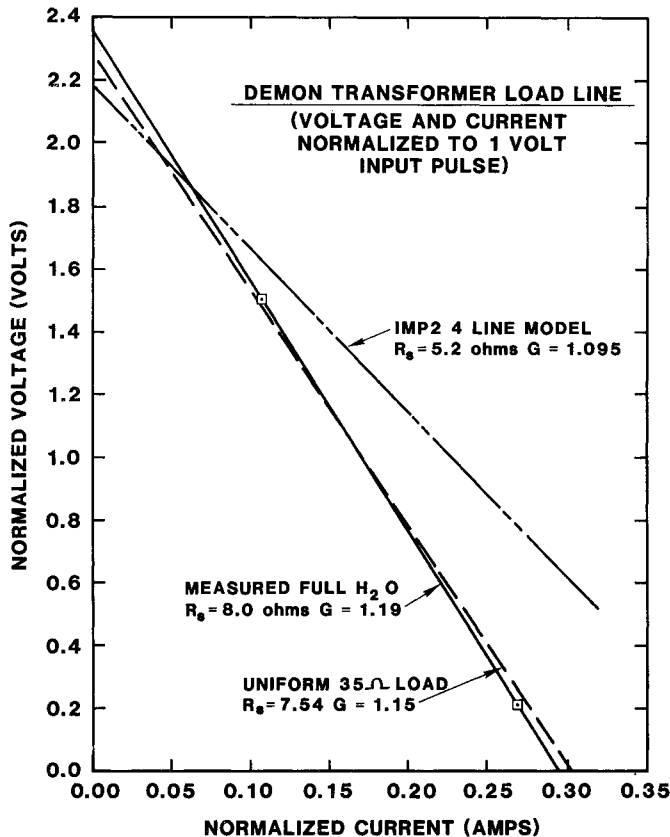


Figure 6.

We have constructed a brass-plate 18 line, one fifth scale model, of the output transformer section of PBFA II to look at voltage addition and energy transport to the vacuum diode load in the full three dimensional geometry. The vacuum region is simulated with a single biconic disk transmission line in air. The experiments consisted of using a 1/5 time-scaled Demon-like input pulse shape and measuring the voltages and currents for central loads of 100, 10, and 5 ohms and for a short circuit. The forward going waveforms in the input flat-plate region were used as a reference and the load waveforms were analyzed to give the Thevenin equivalent source impedance, open circuit voltage, and load inductance. The calculated source impedance is 4.4 ohms with an inductance of 115 nH outside the stack for one half of PBFA II. The one-fifth scale model measurements predict 3.75 MJ of forward going energy will be delivered, by the 36 pulse power modules, into the vacuum region of PBFA II.

Results of the 1/5 scale model experiments indicate that there are no three dimensional problems associated with the PBFA II voltage addition geometry beyond the higher-order mode losses already measured in Demon. The system efficiency, from the scale model and Demon results, is shown to be about 67% from the coaxial module output to the vacuum plasma erosion switch location. The circuit characterization, from these results, is incorporated into an overall circuit model to be used in optimizing PBFA II power flow and diode design¹².

PBFA II Marx and Water Section Computer Model

The models developed for the gas switch region and the transformers have been incorporated into a complete simulation of the PBFA II module through the output of the transmission-line transformers. The model is set up for use with the SCREAMER code on a VAX computer. The SCREAMER upper and lower transformer forward-going voltage waveforms are shown in Figures 7 and 8. All switch times and amplitudes have been set to match Demon operating parameters. Two simulation outputs are shown in Figures 7 and 8.

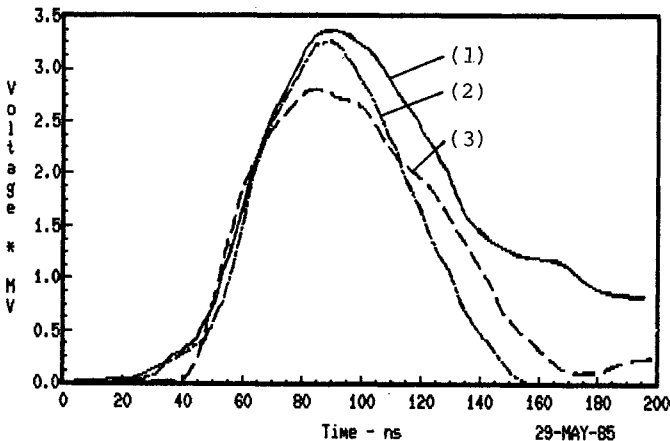


Figure 7. Upper transformer forward-going voltage: 1) SCREAMER model, 2) model with prepulse shield losses, and 3) measured Demon waveform.

The first curve in each figure assumes no additional energy loss mechanism. The second curve in each case adds a loss due to an assumed flashover to the final pre-pulse shield shown in Figure 1. The flashover inductance and resistance are 90 nH and 0.25 ohms for an assumed 6 cm water switch channel. This flashover can be seen in open-shutter photographs, but has not been time resolved. The final curve in each figure is the calculated forward going voltage waveform for a particular Demon experimental shot. The best

agreement is with the assumed flashover loss mechanism. The additional loss seen in the upper waveform may be due to dC/dt effects of streamers in the crossover assemblies, also shown in open shutter photographs. Figure 9 presents the predicted forward-going energy into the PBFA II vacuum region. Curves 1 and 2 are the scaled computer and 18-line simulation results, while curve 3 is scaled from the Demon experimental results.

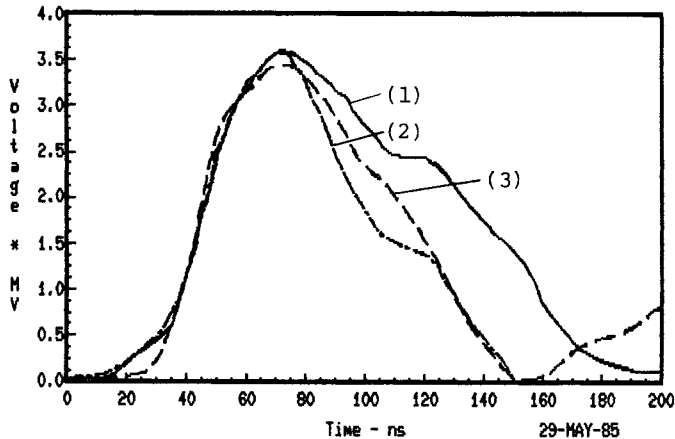


Figure 8. Lower transformer forward-going voltage:
1) SCREAMER model, 2) model with prepulse shield losses, and 3) measured Demon waveform.

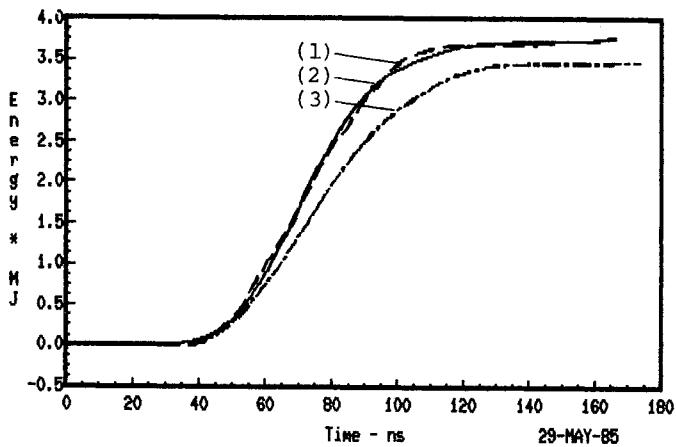


Figure 9. Predicted PBFA II forward-going energy:
1) from scale model, 2) from SCREAMER model, and 3) scaled from Demon output.

Acknowledgements

The authors gratefully acknowledge the continued interest, support, and helpful discussions with T. H. Martin and B. N. Turman. We also wish to thank D. B. Seidel, M. M. Widner and M. L. Kieffer for their help with code development and the Demon experimental team for their work in acquiring data presented in this paper.

References

1. B. N. Turman, J. F. Seamen, E. L. Neau, and D. R. Humphreys, "Development of the Pulse Compression Section for PBFA II," 16th Modulator Symposium, Arlington, VA, June 17-21, 1984.
2. L. X. Schneider, "Development of a High Reliability 6.0 MV, 390 kJ Marx Generator, Proc. 4th IEEE Pulsed Power Conference, Albuquerque, NM, June 6-8, 1983.
3. R. Adams, D. R. Humphreys, J. Woodworth, D. L. Green, and J. F. Seamen, "Ultraviolet Laser Triggering of the 6 MV PBFA II Gas Switch," 16th Modulator Symposium, Arlington, VA, June 17-21, 1984.
4. I. Smith, "Rapid Charging of Transmission Lines," Pulse Sciences, Inc., Oakland, CA, Interim Report, Sandia National Laboratories, April, 1981.
5. P. W. Spence, Y. G. Chen, G. Frazier, and H. Calvin, "Inductance and Resistance of Single-site Water Switches," Proc. 2nd Int'l Pulsed Power Conference, Lubbock, TX, June 12-14, 1979.
6. J. D. Shipman, "A Study of Power and Energy in AMP," Naval Research Laboratories Memo Report, November 1979.
7. J. C. Bowers, and S. R. Sedore, SCEPTRE, A Computer Program For Circuit and Systems Analysis, Englewood Cliffs, New Jersey: Prentice Hall, 1971.
8. S. Sackett, "JASON, A Code for Solving General Electrostatic Problems," UCID-17814, June 1978.
9. E. L. Neau, T. L. Woolston, and K. J. Penn, "Comet-II, A Two-Stage Magnetically Switched Pulsed-Power Module," 16th Modulator Symposium, Arlington, VA, June 17-21, 1984.
10. D. B. Seidel, Sandia National Laboratories, private communications.
11. M. Widner and M. L. Kieffer, Sandia National Laboratories, private communication.
12. D. H. McDaniel, "Design and Optimization of the PBFA II Vacuum Interface and Transmission Lines for Light Ion Fusion," to be presented at 5th IEEE Pulsed Power Conference, Arlington, VA, June 10-12, 1985.

Conclusion

We have presented results of energy transport measurements on the Demon single-line module and on a one-fifth scale 18-line model of PBFA II. Computer simulations of the Demon module show agreement with the experimental measurements and indicate a predicted forward going energy, at the PBFA II vacuum insulator stack, of 3.75 MJ. Differences in the simulation and experimental results show that the ± 10 percent energy output variations and low upper transformer output, observed in Demon, may be due to correctable breakdown problems. Additional analysis is required to accurately model the coupled output transformers. The proposed parallel loss mechanism for the transformers adequately models the forward going energy, but will not correctly interact with vacuum region models. The agreement between the Demon and one-fifth scale model measurements and the computer simulations show that the Demon module design will meet the output requirements for the PBFA II water section.